Electronic Supplementary Information

Experiment Section

Materials: Sodium nitrate ($NaNO_3$, 99.0%), sodium nitrite ($NaNO_2$, 99.0%), ammonium chloride (NH_4Cl), sodium hydroxide (NaOH), sodium salicylate ($C_7H_5NaO_3$), trisodium citrate dihydrate ($C_6H_5Na_3O_7 \cdot 2H_2O$), p-dimethylaminobenzaldehyde ($C_9H_{11}NO$), sodium nitroferricyanide dihydrate ($C_5FeN_6Na_2O \cdot 2H_2O$), 0.8 wt% sulfamic acid solution (H_3NO_3S), sodium hypochlorite solution (NaClO), sulfur powder (S), and Cobalt nitrate hexahydrate ($Co(NO_3)_2 \cdot 6H_2O$) were purchased from Aladdin Ltd. (Shanghai, China). Phosphoric acid (H_3PO_4), hydrochloric acid (HCl), and N-(1-naphthyl)ethylenediamine dihydrochloride were bought from Keshi Chemical Reagent Co. Titanium plate (TP) was purchased from Qingyuan Metal Materials Co., Ltd (Xingtai, China). All reagents used in this work were analytical grade without further purification.

Preparation of $CoS_2@TiO_2$/TP: Firstly, the well-cut small pieces (2.0 × 4.0 cm²) titanium plates were sonicated in acetone, ethanol, and distilled water for 15 min, respectively. Then, the pre-treated TP was put into 40 mL of 5 M NaOH aqueous solution in a Teflon-lined autoclave and heated at 180 °C for 24 h to obtain $Na_2Ti_2O_5$. After cooling down to room temperature, the samples were moved out, washed with deionized water and ethanol several times, and dried at 60 °C for 30 min. Then the synthetic sample was immersed in 0.25 M $Co(NO_3)_2 \cdot 6H_2O$ for 1 h to exchange Na^+ with Co^{2+}, followed by rinsing several times with deionized water and dried overnight at 60 °C. Subsequently, $CoTi_2O_5$ was annealed in a tube furnace with S powder (0.2 g) at 500 °C under an argon atmosphere for 2 h. After cooling to room temperature, $CoS_2@TiO_2$/TP was finally obtained.

Preparation of TiO_2/TP: Pristine TiO_2/TP nanobelts array was synthesized using the same methods but with 1 M HCl for ion-exchange. The as-prepared $H_2Ti_2O_5 \cdot H_2O$ was then washed with distilled water and ethanol several times and dried at 60 °C for 30 min. Subsequently, $H_2Ti_2O_5 \cdot H_2O$ was annealed in a tubular furnace at 500 °C under an argon atmosphere for 2 h. After cooling to room temperature, TiO_2/TP was finally

obtained.

Preparation of CoS$_2$/TP: Briefly, 1 mmol of Co(NO$_3$)$_2$·6H$_2$O and 4 mmol of L-cysteine were dispersed in 30 mL of deionized water under constant stirring, followed by a hydrothermal reaction at 200 °C for 12 h. After rinsed thoroughly and dried overnight, the CoS$_2$ nanoparticles were obtained. Finally, CoS$_2$ ink was prepared by mixing the CoS$_2$ powder with sopropyl alcohol and Nafion (5 wt%) (v/v = 24/1) to achieve a catalyst concentration of 10 mg mL^{-1} via sonication for 60 min, then 40 μL of uniform catalyst ink was coated on a 0.25 cm^2 TP (mass loading of CoS$_2$: 1.60 mg cm^{-2}) and dried in air.

Characterizations: The crystal structure of as-prepared materials was identified through X-ray diffraction (XRD, Philip D8). Scanning electron microscopy (SEM, ZISS 300) and transmission electron microscopy (TEM, JEM-F200, JEOL Ltd.) were carried out to reveal the morphology information of samples. Energy dispersive X-ray (EDX) and X-ray photoelectron spectroscopy (XPS, ESCALAB 250 Xi) were utilized to analyze chemical compositions. The absorbance data of spectrophotometer was acquired on Ultraviolet-visible (UV) spectrophotometer (Shimadzu UV-2700). Gas chromatography (GC-2014C, SHIMADZU) was utilized to quantitatively detect H$_2$. ^{1}H NMR spectra were collected on Varian VNMRS 600 MHz (the USA).

Electrochemical measurements: All electrochemical measurements were implemented in an H-type cell separated by a treated Nafion 117 membrane using a CHI 760E electrochemical workstation (Shanghai, Chenhua). Electrolyte solution (35 mL) was Ar-saturated 0.1 M NaOH with and without 0.1 M NO$_3^-$ (NaNO$_3$), using CoS$_2$@TiO$_2$/TP (0.5 × 0.5 cm^2, mass loading of CoS$_2$: 1.58 mg cm^{-2}), Pt, and Hg/HgO as the working electrode, counter electrode, and reference electrode, respectively. Before the stability test, a thin tube was inserted into H-cell and fixed below the electrolyte level. At each sampling time, 0.2 mL of electrolyte was pipetted into the centrifugal tube for subsequent testing. According to the Nernst equation, all the potentials were converted into the potential of the reversible hydrogen electrode (RHE) ($E_{RHE} = E_{Hg/HgO}$ + 0.059 × pH + 0.098 V), and the current density was normalized by the geometric surface area.

Determination of NH$_3$: The yields of NH$_3$ in the electrolyte were calculated by spectrophotometer using the indophenol blue method.[1] Concretely, 2 mL of the collected electrolyte after electrolysis mixed with 2 mL of 1 M NaOH solution containing 5% salicylic acid and 5% sodium citrate. Then, 1 mL of 0.05 M NaClO and 200 μL of 1 wt% sodium nitroferricyanide dihydrate were dropped in the collected electrolyte solution. The electrolytes of different potential and cycle tests were diluted 20 times, and the electrolytes of stability tests were diluted 200 times in H-cell. After maintained in the dark for 2 h, the concentration of NH$_3$ was identified by UV spectroscopy for a certain wavelength about 655 nm:

$$NH_3 \text{ yield} = [NH_3] \times V / (17 \times t \times A)$$

Where [NH$_3$] is the mass concentration, V is the volume of the cathodic reaction electrolyte, t is the reduction time, and A is the area of the working electrode.

$$FE = (n \times F \times c \times V) / (M \times Q)$$

Where F is the Faraday constant, n is the electrons transfer number, c is the calculated products concentration, V is the volume of the cathodic reaction electrolyte, M is the molecular mass of products, and Q is the total charge during electrosynthesis.

Determination of NO$_2^-$: The NO$_2^-$ concentration was detected by the Griess test using UV spectrophotometry.[2] The Griess reagent was provided through adding N-(1-naphthyl)ethylenediamine dihydrochloride (0.1 g), sulfanilamide (1.0 g), and H$_3$PO$_4$ (2.94 mL) in 50 mL H$_2$O. Typically, 1.0 mL Griess reagent was added to 1.0 mL electrolyte and 2.0 mL H$_2$O. The electrolytes of different potential were diluted 2 times. After maintained for 10 min, the concentration of NO$_2^-$ was measured by UV spectroscopy at a wavelength of 540 nm.

Determination of N$_2$H$_4$: The Watt and Chrisp's method[3] was used to assess whether N$_2$H$_4$ formed during the NO$_3^-$RR process. The chromogenic reagent was prepared through mixing 5.99 g p-dimethylaminobenzaldehyde, 30 mL concentrated HCl, and 300 mL ethanol. The absorbance at 460 nm was measured to quantify the N$_2$H$_4$ concentration using standard N$_2$H$_4$ solutions.

Determination of H$_2$: Detection and quantification of H$_2$ was executed on a

Shimadzu GC-2014C gas chromatograph system equipped with thermal conductivity detector (TCD) and online auto-sampling system.

NO₃⁻ isotopic labelling experiment: The generated NH_3 was verified by an isotope-labelled tracer experiment using 0.1 M $^{15}NO_3^-$ as a N source. After 1 h of electroreduction at −0.7 V, the electrolyte (2 mL) in the cathodic chamber was neutralized by HCl aqueous solution (1.2 M). After that, the neutralized electrolyte (500 μL) was mixed with deuterium oxide (D_2O, 50 μL). And the mixture was sealed into a nuclear magnetic resonance (NMR) tube (5 mm in diameter, 600 MHz) for further tests.
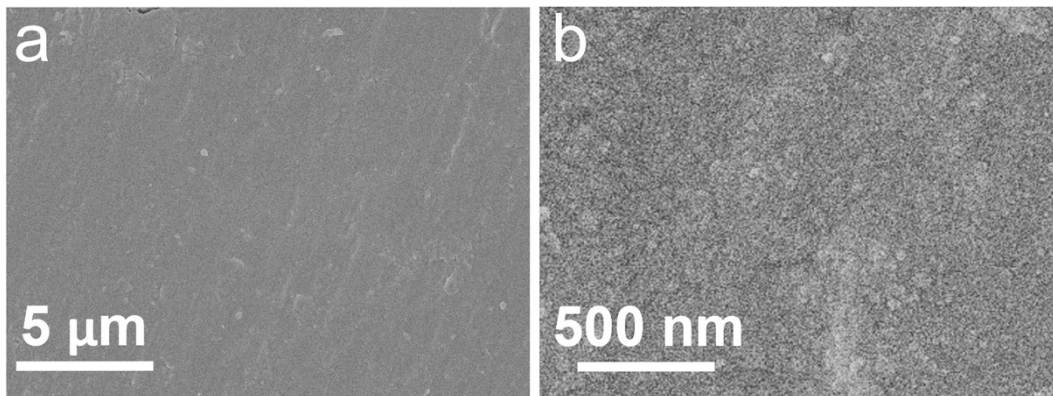
Fig. S1. SEM images of bare TP.
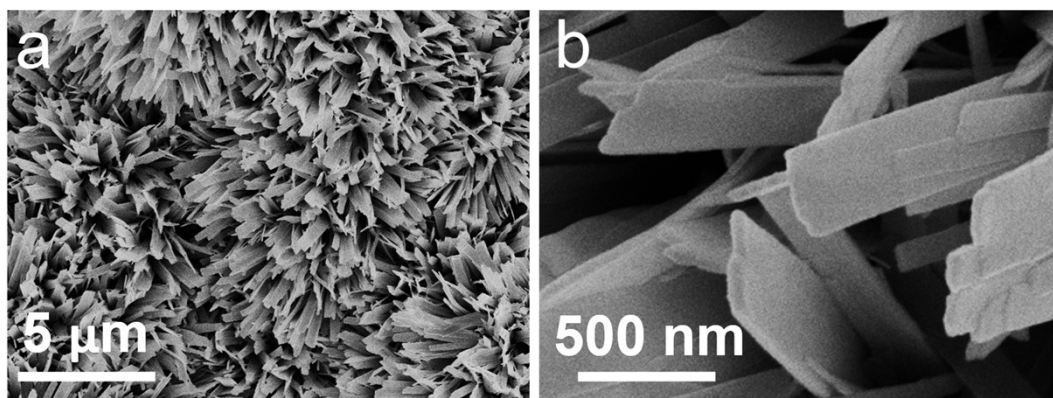
Fig. S2. SEM images of Na-titanate on TP.
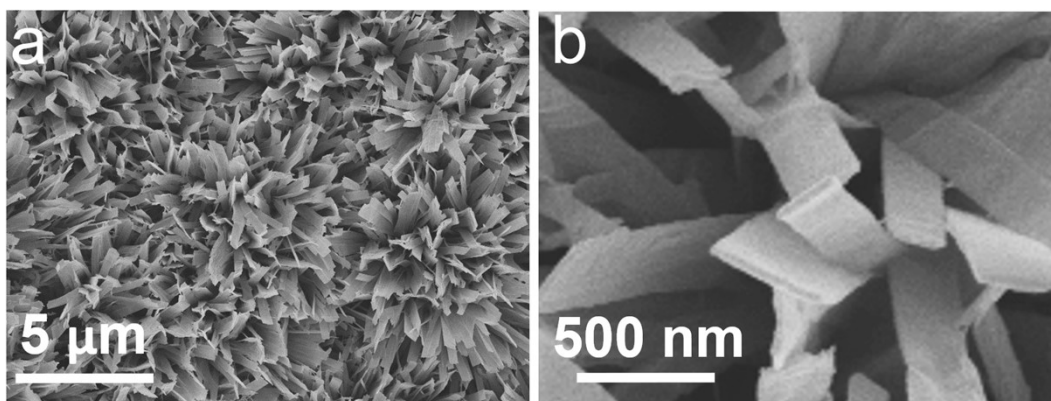
Fig. S3. SEM images of Co-titanate on TP.
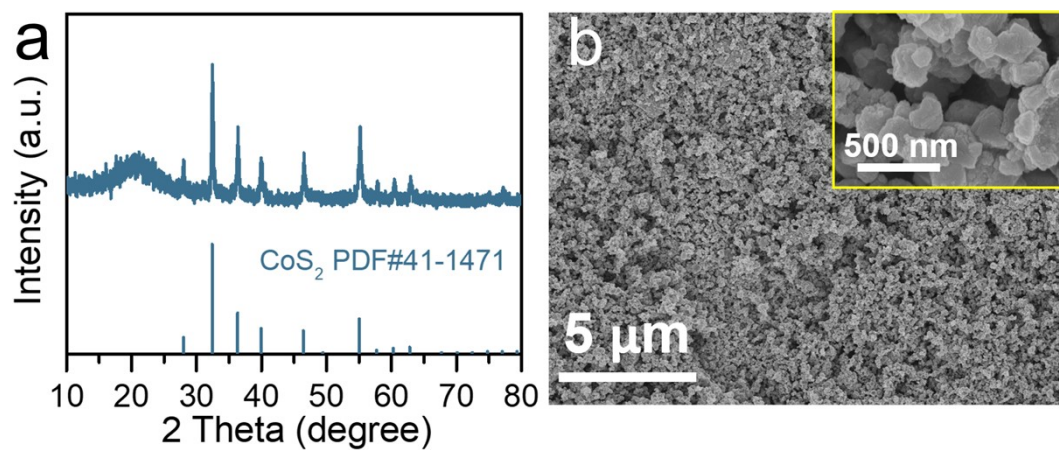
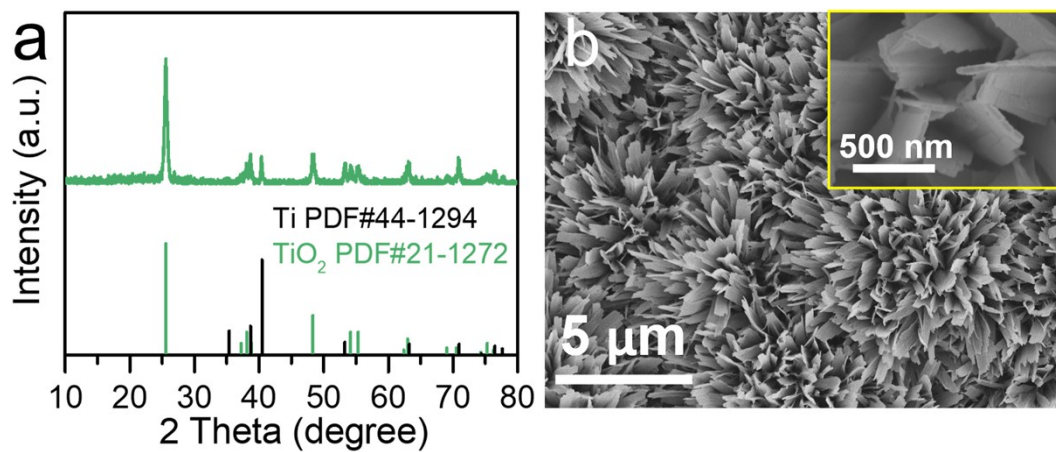**Fig. S4.** (a) XRD pattern and (b) SEM images of CoS_2 nanoparticles.

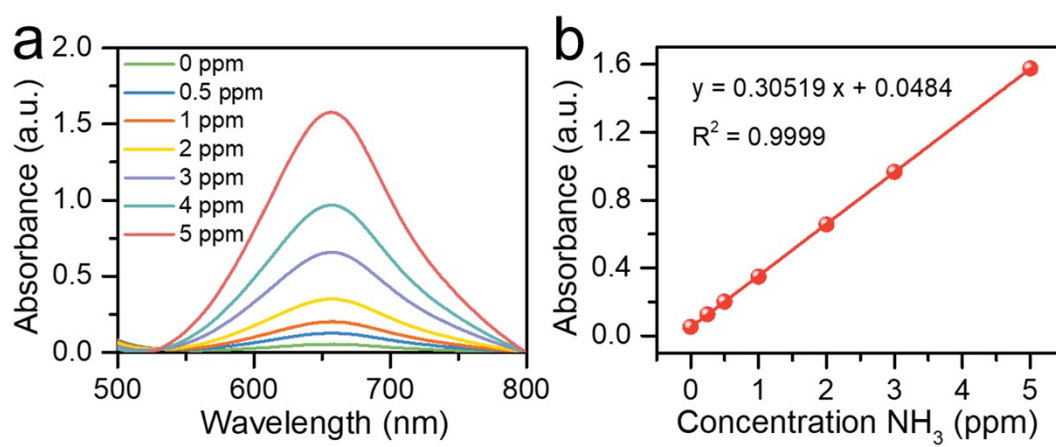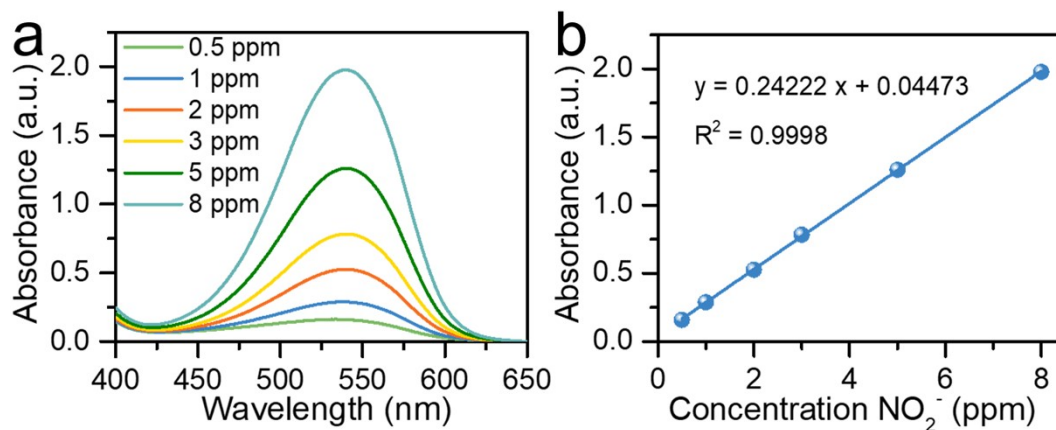**Fig. S5.** (a) XRD pattern and (b) SEM images of TiO$_2$/TP.

Fig. S6. (a) UV-Vis absorption spectra and (b) corresponding calibration curve used for calculation of NH$_3$ concentration.

Fig. S7. (a) UV-Vis absorption spectra and (b) corresponding calibration curve used for calculation of NO_2^- concentration.
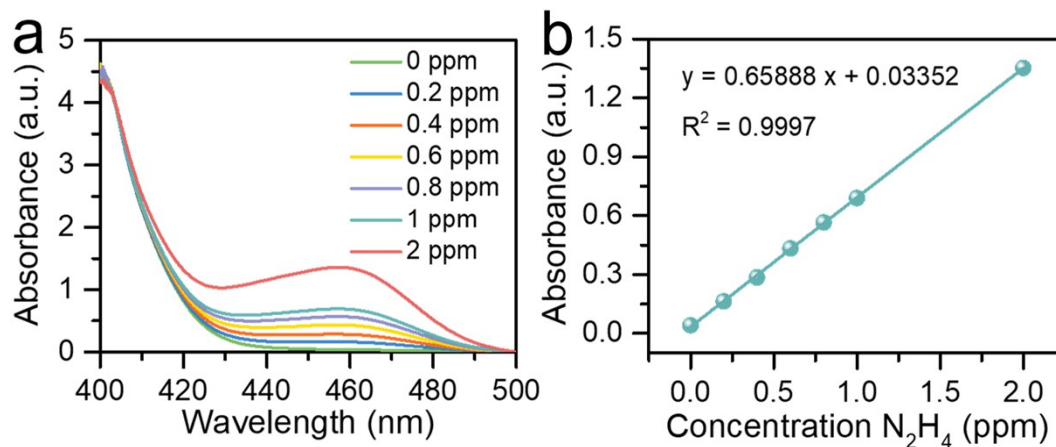

Fig. S8. (a) UV-Vis absorption spectra and (b) corresponding calibration curve used for calculation of N_2H_4 concentration.
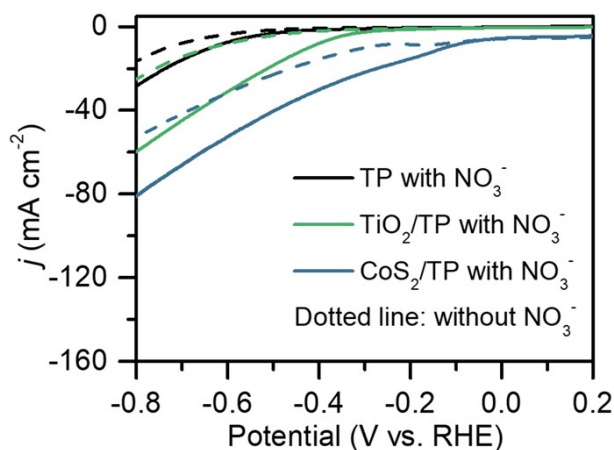
Fig. S9. LSV curves of TP, TiO$_2$/TP, and CoS$_2$/TP in 0.1 M NaOH with and without 0.1 M NO$_3^-$.
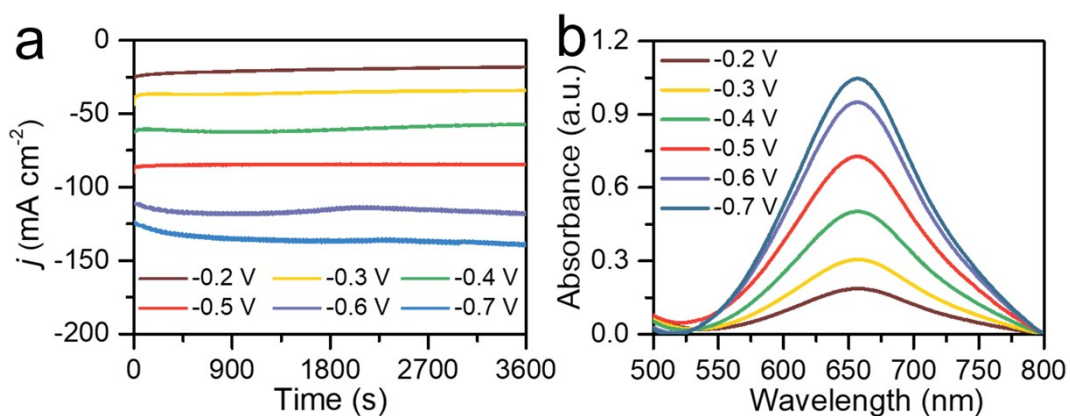

Fig. S10. (a) Chronoamperometry curves of CoS$_2$@TiO$_2$/TP at each given potential and (b) corresponding UV-Vis absorption spectra of the electrolytes for calculation of NH$_3$ concentration.
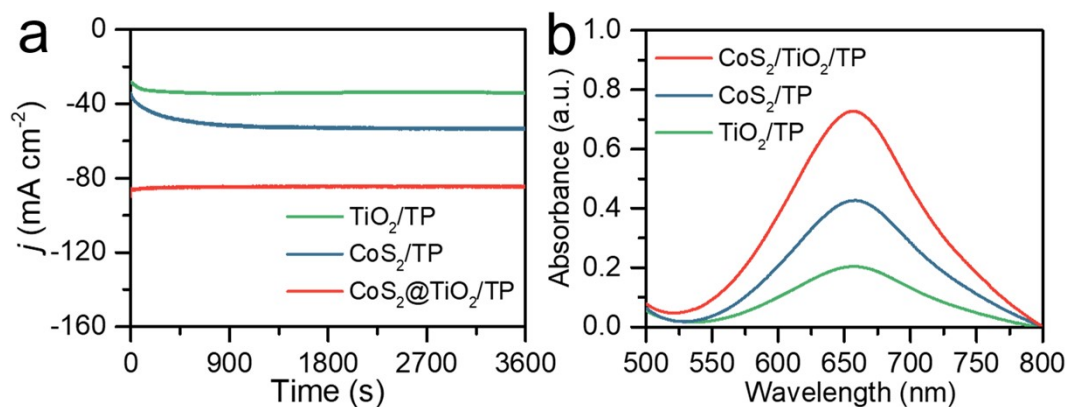
Fig. S11. Time-dependent current density curves of TiO$_2$/TP, CoS$_2$/TP, and CoS$_2$@TiO$_2$/TP for the NO$_3^-$RR at −0.5 V and (b) corresponding UV-Vis absorption spectra of the electrolytes for calculation of NH$_3$ concentration.
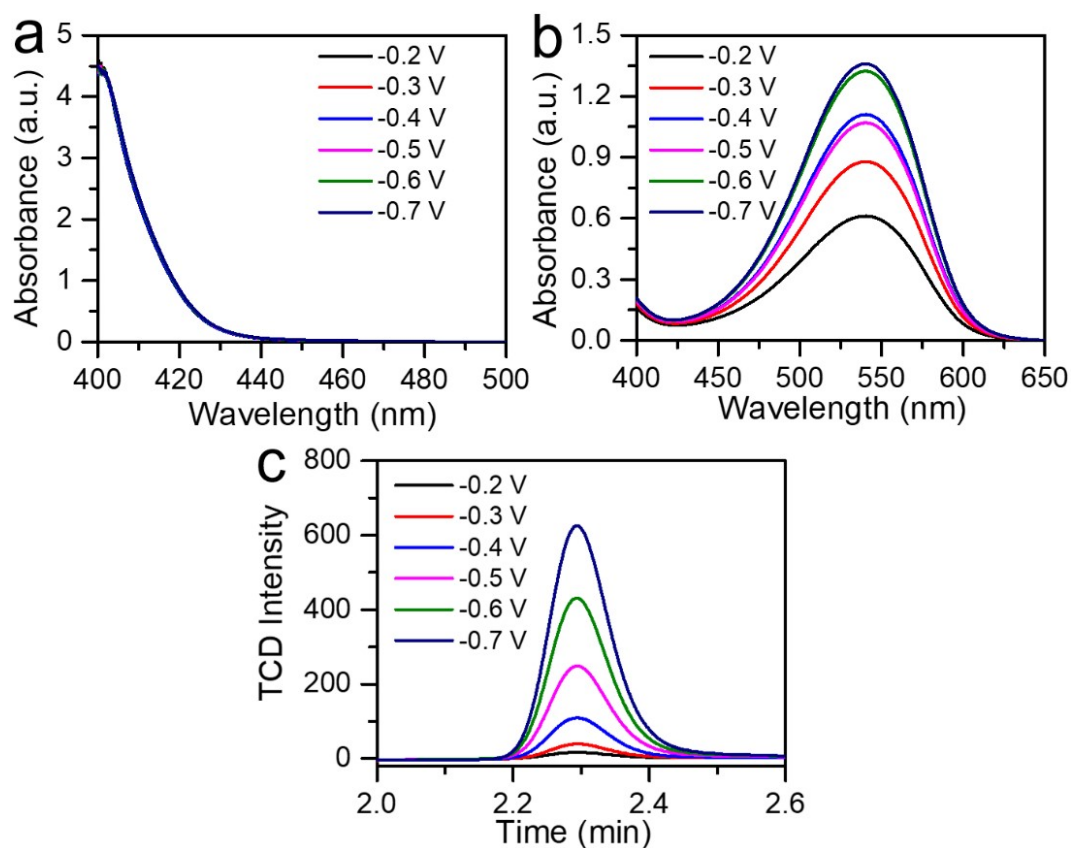

Fig. S12. UV-Vis absorption spectra of produced (a) N$_2$H$_4$ and (b) NO$_2^-$. (c) Chromatograph curves of H$_2$ detected by GC at each given potential.
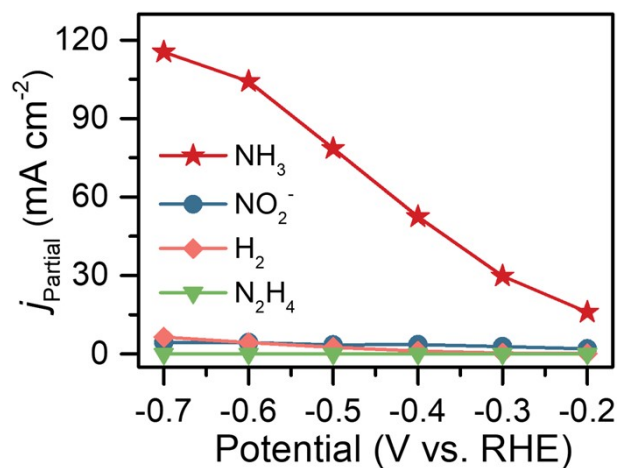
Fig. S13. Partial current densities of NH_3, NO_2^-, H_2, and N_2H_4 for $CoS_2@TiO_2/TP$ at different potentials.
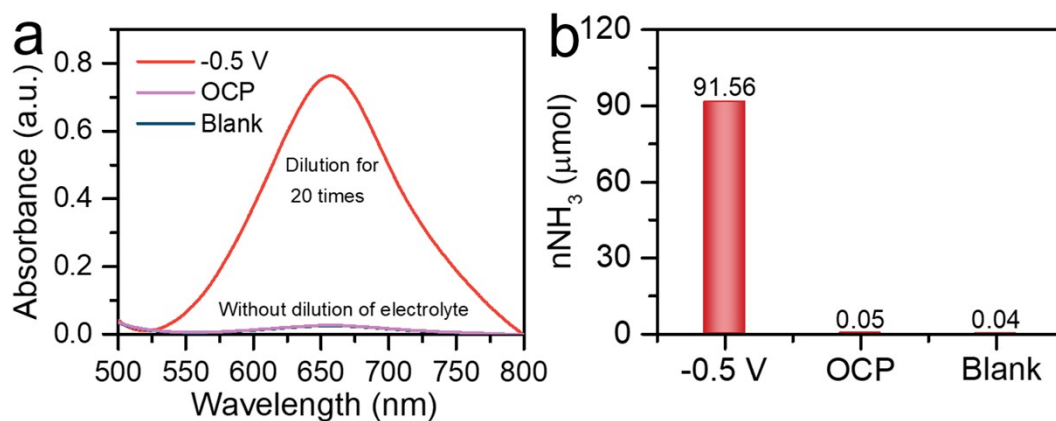

Fig. S14. (a) UV spectra and (b) comparison of the amount of produced NH_3 of $CoS_2@TiO_2/TP$ for the NO_3^-RR at different conditions.
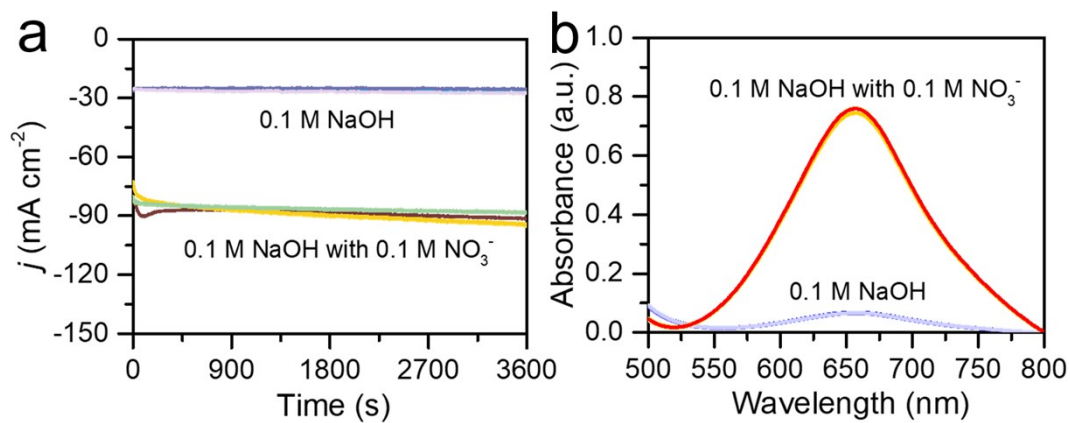
Fig. S15. (a) Chronoamperometry curves and (b) corresponding UV-Vis absorption spectra of $CoS_2@TiO_2/TP$ for during the alternating cycles tests between 0.1 M NaOH with and without 0.1 M NO_3^-.

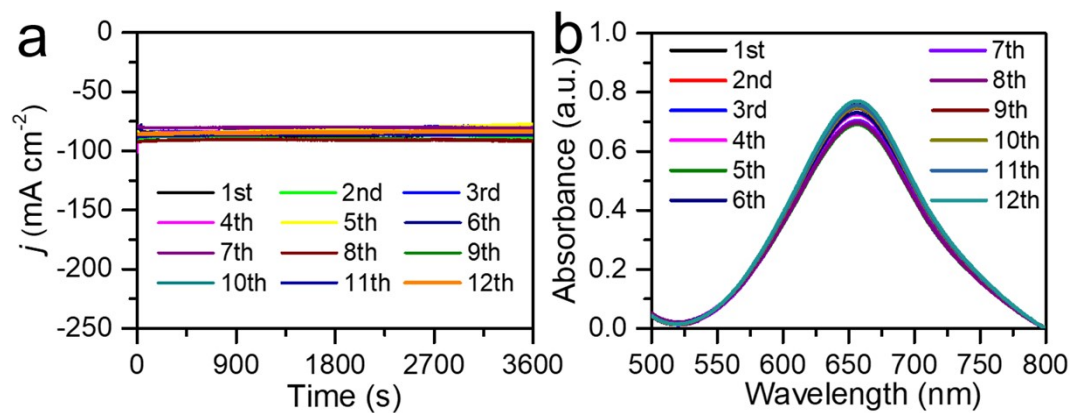**Fig. S16.** (a) Chronoamperometry curves for $CoS_2@TiO_2/TP$ during recycling tests toward NO_3^-RR at –0.5 V and (b) corresponding UV-Vis absorption spectra for electrogenerated NH_3.
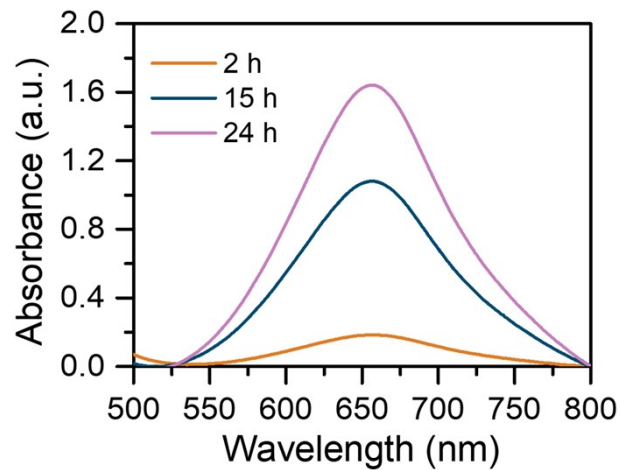
Fig. S17. UV-Vis absorption spectra of electrogenerated NH_3 for $CoS_2@TiO_2$/TP at different time electrolysis during long time electrolysis.
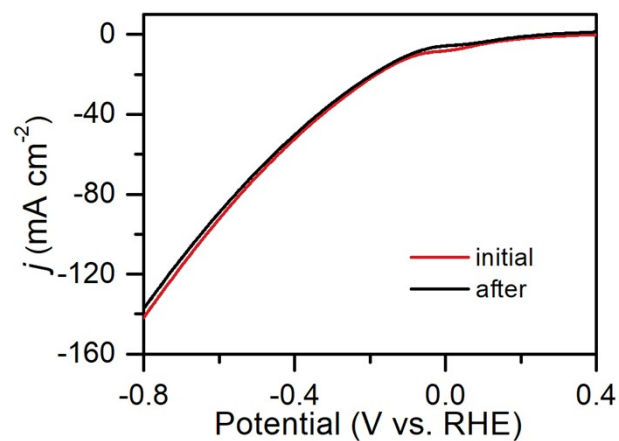
Fig. S18. LSV curves of $CoS_2@TiO_2$/TP before and after stability test.
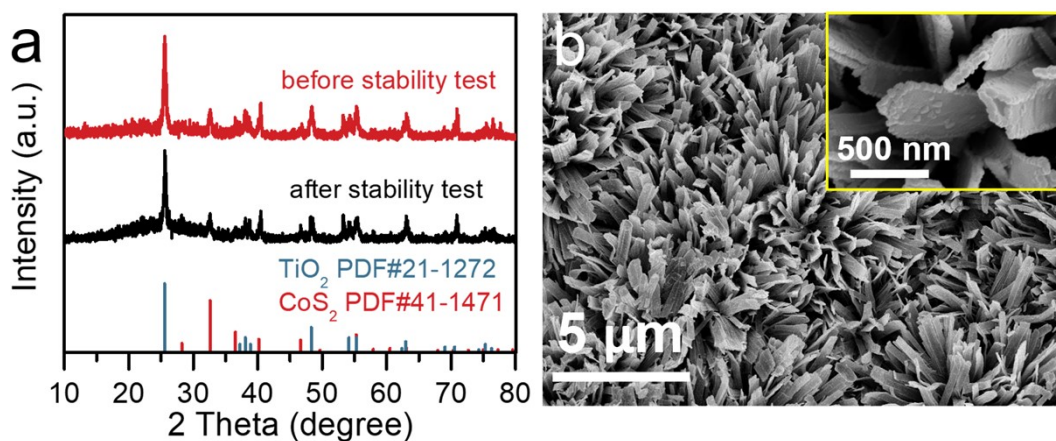
Fig. S19. (a) XRD patterns of CoS$_2$@TiO$_2$/TP before and after long-term electrolysis. (b) SEM images of CoS$_2$@TiO$_2$/TP after long-term electrolysis.

Fig. S20. XPS spectra in the (a) Co 2p, (b) S 2p, (c) Ti 2p, and (d) O 1s regions of CoS$_2$@TiO$_2$ after electrolysis.

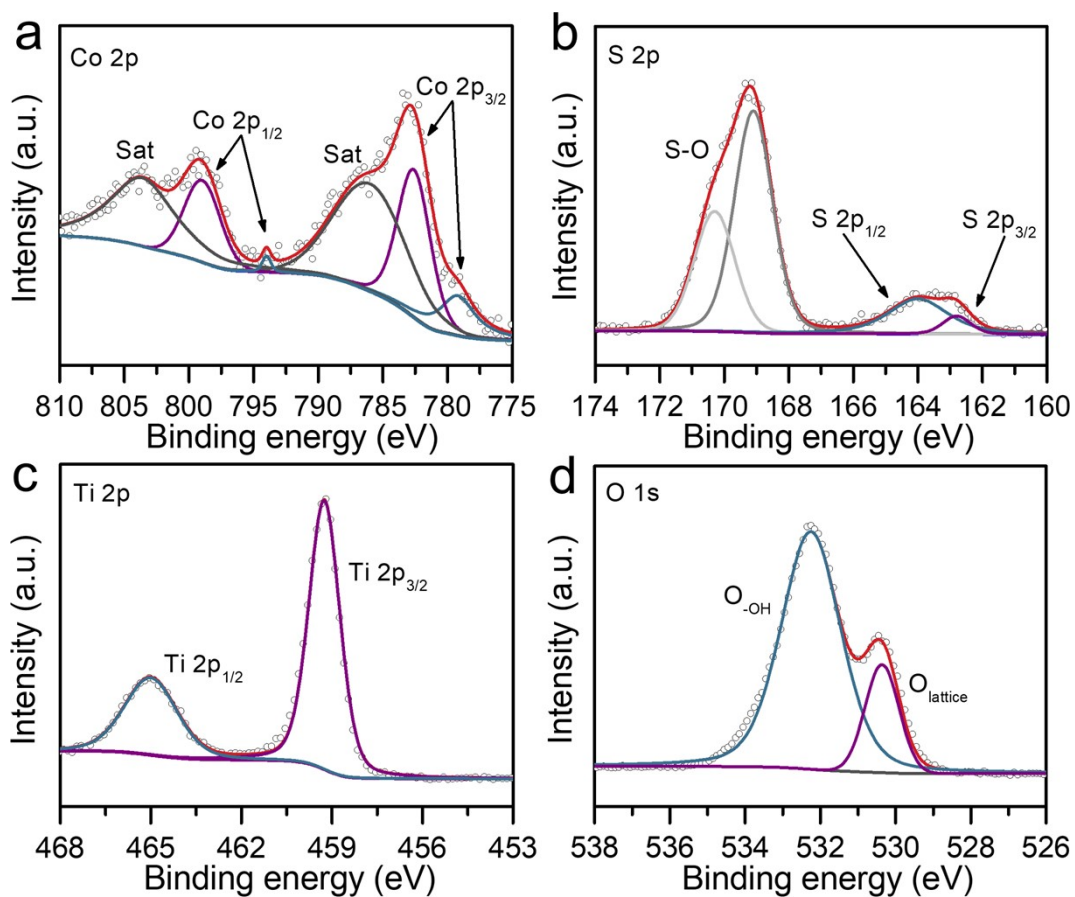**Table S1** Comparison of the FE and NH_3 yield for $CoS_2@TiO_2/TP$ with other reported NO_3^-RR electrocatalysts.

Catalyst	Electrolyte	NH_3 yield (μmol h^{-1} cm^{-2})	FE (%)	Potential (V vs. RHE)	Ref
$CoS_2@TiO_2/TP$	0.1 M NaOH (0.1 M NO_3^-)	538.21	85.14	–0.70	This work
		366.24	92.80	–0.50	
PTCDA/O-Cu	0.1 M PBS (500 ppm NO_3^-)	25.65	85.90	–0.40	4
Cu_3P NA/CF	0.1 M PBS (0.1 M NO_3^-)	49.88	62.9	–0.60	5
pCuO-5	0.05 M H_2SO_4 (0.05 M NO_3^-)	290.00	80.00	–0.60	6
TiO_{2-x}	0.5 M Na_2SO_4 (50 ppm NO_3^-)	45.00	85.00	–0.40	7
NiPc complex	0.1 M KOH (NO_3^-)	–	85.00	–0.40	8
Cu	1 M NaOH (0.1 M $NaNO_3$)	–	79.00	–0.50	9
$Cu_{50}Ni_{50}$/PTFE	1 M KOH (10 mM NO_3^-)	–	84.00	–0.05	10
Ti/GC	0.1 M HNO_3 (0.3 M NO_3^-)	–	82.00	–1.00	11
Cu/Cu_2O NWAs	0.5 M Na_2SO_4 (200 ppm NO_3^-)	244.90	95.80	–0.85	12
Co/CoO NSA	0.1 M Na_2SO_4 (200 ppm NO_3^-)	194.46	93.80	–0.65	13
Ru-ST-0.6	1 M KOH (1 M NO_3^-)	1170.00	~100	−0.20	14
Au/C	0.5 M K_2SO_4 (1 mM KNO_3)	1.58	26.00	−0.30	15
Pd/TiO_2	1 M LiCl (0.25 M NO_3^-)	66.00	92.10	−0.70	16
In-S-G	0.1 M KOH (0.1 M NO_3^-)	74.82	75.00	–0.50	17
Fe-PPy SACs	0.1 M KOH (0.1 M NO_3^-)	161.71	~100	−0.70	18
Fe-Co_3O_4 NA/TM	0.1 M PBS (50 mM NO_3^-)	38.17	95.50	−0.70	19
PP-Co/CP	0.1 M NaOH (0.1 M NO_3^-)	220.00	90.10	−0.60	20

References

1   D. Zhu, L. Zhang, R. E. Ruther and R. J. Hamers, *Nat. Mater.*, 2013, **12**, 836–841.

2   L. C. Green, D. A. Wagner, J. Glogowski, P. L. Skipper, J. S. Wishnok and S. R. Tannenbaum, *Anal. Biochem.*, 1982, **126**, 131–138.

3   G. W. Watt and J. D. Chrisp, *Anal. Chem.*, 1952, **24**, 2006–2008.

4   G. Chen, Y. Yuan, H. Jiang, S. Ren, L. Ding, L. Ma, T. Wu, J. Lu and H. Wang, *Nat. Energy*, 2020, **5**, 605–613.

5   J. Liang, B. Deng, Q. Liu, G. Wen, Q. Liu, T. Li, Y. Luo, A. A. Alshehri, K. A. Alzahrani, D. Ma and X. Sun, *Green Chem.*, 2021, **23**, 5487−5493.

6   R. Daiyan, T. Tran-Phu, P. Kumar, K. Iputera, Z. Tong, J. Leverett, M. H. A. Khan, A. Asghar Esmailpour, A. Jalili, M. Lim, A. Tricoli, R. Liu, X. Lu, E. Lovell and R. Amal, *Energy Environ. Sci.*, 2021, **14**, 3588–3598.

7   R. Jia, Y. Wang, C. Wang, Y. Ling, Y. Yu and B. Zhang, *ACS Catal.*, 2020, **10**, 3533–3540.

8   N. Chebotareva and T. Nyokong, *J. Appl. Electrochem.,* 1997, **27**, 975–981.

9   D. Reyter, G. Chamoulaud, D. Bélanger and L. Roué, *J. Electroanal. Chem.*, 2006, **596**, 13–24.

10 Y. Wang, A. Xu, Z. Wang, L. Huang, J. Li, F. Li, J. Wicks, M. Luo, D. H. Nam, C. S. Tan, Y. Ding, J. Wu, Y. Lum, C. T. Dinh, D. Sinton, G. Zheng and E. H. Sargent, *J. Am. Chem. Soc.*, 2020, **142**, 5702–5708.

11 J. M. McEnaney, S. J. Blair, A. C. Nielander, J. A. Schwalbe, D. M. Koshy, M. Cargnello and T. F. Jaramillo, *ACS Sustain. Chem. Eng.*, 2020, **8**, 2672–2681.

12 Y. Wang, W. Zhou, R. Jia, Y. Yu and B. Zhang, *Angew. Chem. Int. Ed.*, 2020, **59**, 5350–5354.

13 Y. Yu, C. Wang, Y. Yu, Y. Wang and B. Zhang, *Sci. China Chem.*, 2020, **63**, 1469–1476.

14 J. Li, G. Zhan, J. Yang, F. Quan, C. Mao, Y. Liu, B. Wang, F. Lei, L. Li, A. W. M. Chan, L. Xu, Y. Shi, Y. Du, W. Hao, P. K. Wong, J. Wang, S. Dou, L. Zhang and J. C. Yu, *J. Am. Chem. Soc.*, 2020, **142**, 7036–7046.

15   J. Choi, H. L. Du, C. K. Nguyen, B. H. R. Suryanto, A. N. Simonov and D. R. MacFarlane, *ACS Energy Lett.*, 2020, **5**, 2095–2097.

16   Y. Guo, R. Zhang, S. Zhang, Y. Zhao, Q. Yang, Z. Huang, B. Dong and C. Zhi, *Energy Environ. Sci.*, 2021, **14**, 3938–3944.

17   F. Lei, W. Xu, J. Yu, K. Li, J. Xie, P. Hao, G. Cui and B. Tang, *Chem. Eng. J.*, 2021, **426**, 131317.

18   P. Li, Z. Jin, Z. Fang and G. Yu, *Energy Environ. Sci.*, 2021, **14**, 3522–3531.

19   P. Wei, J. Liang, Q. Liu, L. Xie, X. Tong, Y. Ren, T. Li, Y. Luo, N. Li, B. Tang, A. M. Asiri, M. S. Hamdy, Q. Kong, Z. Wang and X. Sun, *J. Colloid Interf. Sci.*, 2022, **615**, 636–642.

20   Q. Chen, J. Liang, Q. Liu, K. Dong, L. Yue, P. Wei, Y. Luo, Q. Liu, N. Li, B. Tang, A. A. Alshehri, M. S. Hamdy, Z. Jiang and X. Sun, *Chem. Commun.*, 2022, **58**, 4259–4262.